Magnons in two-dimensional spin glasses: The high-field limit

I. Avgin and D. L. Huber
Department of Physics, University of Wisconsin–Madison, Madison, Wisconsin 53706

W. Y. Ching
Department of Physics, University of Missouri–Kansas City, Kansas City, Missouri 64110
(Received 19 April 1993)

The linearized magnetic excitations (magnons) in a two-dimensional $\pm J$ Heisenberg spin glass are investigated in the limit where the field is assumed to be strong enough to set up complete alignment of the ground state. The density of states, the localization indices, and the dynamic structure factor at zero temperature are computed by numerical simulation techniques. A comparison is made between the numerical results for the density of states and the dynamic structure factor and the predictions of the coherent-exchange approximation. Numerical results at zero field are also presented.

I. INTRODUCTION

In a recent paper,[1] we investigated a three-dimensional $\pm J$ Heisenberg spin glass in a strong field using numerical techniques and the coherent-exchange approximation[2] (CEA), a variation of the coherent-potential approximation. The CEA semiquantitatively reproduced the numerical data for the magnon density of states and the dynamic structure factor for a cubic lattice. We also investigated a one-dimensional version of the model which can be connected formally to the electronic disorder problem.[3] Here the CEA quantitatively accounted for the numerical data in the low-energy regime and the exact calculations done for the electronic disorder problem in the weak disorder limit.

In this paper, we study the high-field behavior of the magnons in a two-dimensional $\pm J$ Heisenberg spin glass using numerical simulation techniques and the CEA. The field is assumed to be sufficiently large to align the ground state completely, in contrast to zero field, where the spin glass is known to have a noncollinear frustrated ground state, which makes the problem very hard to cope with using conventional methods. In the high-field limit, the spin-glass system is intermediate in complexity between the spin glass in zero field and the ideal ferromagnet. The investigations reported in this paper are suggested by the work of Shender[4] who used the effective-medium theory to calculate the low-lying collective excitations of the spin glass in the high-field limit. In this paper, we calculate the magnon density of states and the localization indices (or inverse localization lengths), and the dynamic structure factor at zero temperature for the entire spectrum using numerical methods and compare with the predictions of the CEA—which reduces to the effective-medium theory at low energies.

The Heisenberg spin-glass Hamiltonian is written[5]

$$\mathcal{H}=-H\sum_j S_j^z-\sum_{\langle i,j\rangle} J_{ij}\mathbf{S}_i\cdot\mathbf{S}_j\ , \tag{1}$$

where H is the applied field (in units of $g\mu_B$), and $\langle\ \rangle$ implies that summation is over the nearest neighbors. The exchange interactions J_{ij} are independent random variables with a distribution

$$P(J_{ij})=(1-c)\delta(J_{ij}-J)+c\,\delta(J_{ij}+J)\ . \tag{2}$$

The magnon density of states, the localization indices, and the zero-temperature dynamic structure factor in the high-field limit are all defined in Ref. 1. Here, they are presented for a square lattice for $c=0.05$, 0.1, 0.2, 0.3, 0.4, and 0.5 (the results for $c>0.5$ are obtained from the data for $c<0.5$ by reflection about $E=H$). In all cases, $J=S=1$, so that the magnon bandwidth when $c=0$ and 1 is equal to 8. Thus, the magnon energy can take any value between $H-8$ and $H+8$ for a random distribution of the bonds.

II. RESULTS

Here the numerical and the CEA calculations of the density of states, the localization indices, and the zero-temperature dynamic structure factor are presented. Figure 1(a) is a histogram of the magnon density of states for various c values. The data are obtained from 5 configurations of a 24×24 array with periodic boundary conditions. As the concentration increases, the density of states shifts towards the lower edge of the spectrum. That is, the magnons are distributed between H and $H+8$ when $c=0$ and between $H-8$ and H when $c=1$, and they are symmetrically (in the thermodynamic limit) distributed about H when $c=0.5$. For $c<0.5$, there are two main peaks at $E-H=0$ and $E-H=4$ (energy is also measured in units of J); however, the peak at high energy increases as the concentration decreases, while the low-energy peak is not affected by changing the bond concentration. When $c=0$, the peak at $E-H=4$ becomes the logarithmic singularity of the two-dimensional ferromagnet.

The CEA results for the density of states are shown in Fig. 1(b). For a square lattice, we took the site Green's function to have the approximate form[6]

0163-1829/93/48(21)/16109(4)/$06.00

$$\langle G_0(E)\rangle = -1/[8\pi J_c(E)] \times \ln\{[E-H-8J_c(E)]/(E-H)\}\ , \quad (3)$$

where $J_c(E)$ is the coherent-exchange integral characterizing the random medium and is determined self-consistently (see Ref. 1). One is forced to use an approximate expression for the Green's function in order not to accumulate numerical errors when J_c is determined self-consistently. The density-of-states plots clearly predict the shift towards the lower edge of the spectrum as the concentration increased as well as the peak at $E-H=0$. The absence of the peak at $E-H=4$, which is present in the numerical data for $c \leq 0.2$, is a consequence of our having used an approximate Green's function corresponding to a flat density of states, $0 \leq E-H \leq 8$, when $c=0$. For $c=0.5$, the distribution is symmetric about the point $E=H$. The CEA also predicts long tails at both ends of the density of states; however, the tail in the high-energy side of the spectrum is inconsistent with the data.

Figure 2 shows the localization indices L_ν for various values of c for single configurations of 24×24 arrays. For finite number of spins N, the L_ν^{-1} [as defined in Eq. (5) of Ref. 1] is a measure of the number of sites on which the mode has significant amplitude. Thus $L_\nu \sim N^{-1}$ indicates the extended states. For $c=0.05$, the modes where $E-H<0$ are localized, while the other modes are nearly

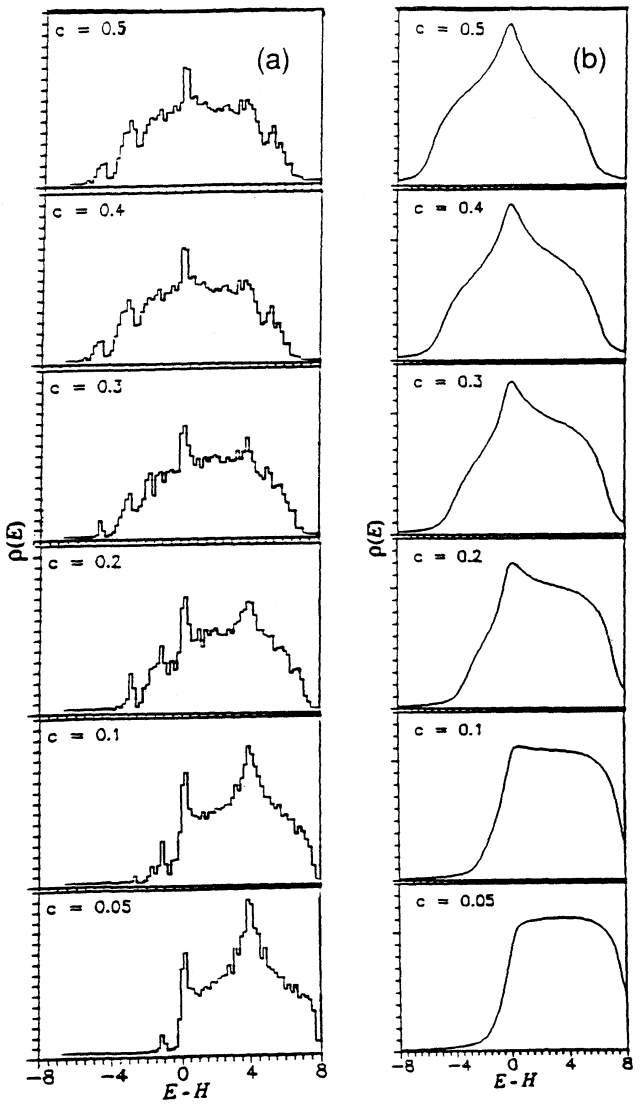

FIG. 1. (a) Histograms of the magnon density of states for the high-field limit for various concentrations. Data are obtained from five configurations of a 24×24 array. All the histograms have the same area. (b) Density of states obtained from the coherent-exchange approximation for various values of c. All curves have the unit area, imaginary part of the energy $\varepsilon=0.5$. The curves are to be compared with the corresponding histograms shown in (a). Energy is measured in units of J ($=S=1$).

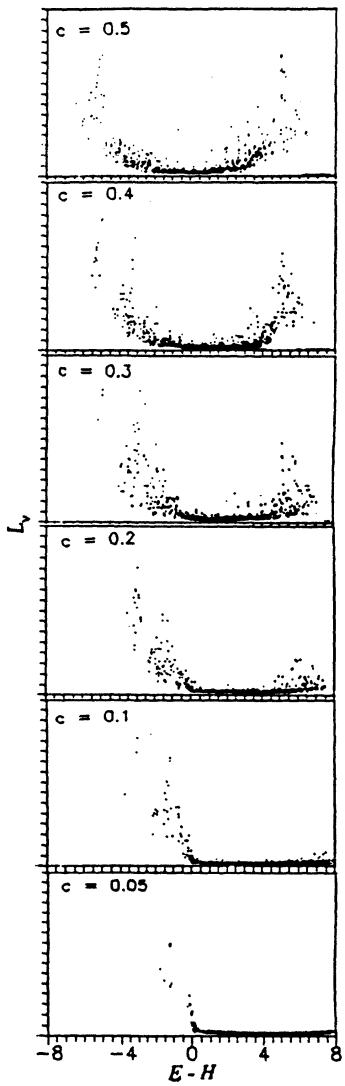

FIG. 2 Localization indices L_ν for various concentrations obtained from a single configuration of a 24×24 array. Similar results are obtained with other configurations. $J=S=1$, and energy is measured in units of J. Vertical scales in all panels are between 0 and 0.4.

localized—a result that is consistent with the findings of Ref. 4. The localized modes also appear at the top of the band as the disorder increases.

The zero-temperature dynamic structure factors for single configurations of 24×24 arrays are shown in Fig. 3(a). The dynamic structures are calculated using Eq. (8) of Ref. 1 with $\alpha=0.5$ in the exponential cutoff factor for the wave vectors $\mathbf{Q}=(\pi/8)(n,n)$ with $n=2$, 4, 6, and 8. The peaks in the dynamic structure factors broaden and move to the lower edge of the spectrum as the negative bond concentration is increased. The broadening of the peaks reflects the fact that $\mathbf{Q}$ is not a good quantum number for systems with no translational invariance. For small concentrations ($c<0.4$), a tail develops on the low-energy side which evolves eventually into a satellite peak at higher concentrations. For $c=0.5$ the peaks are symmetric (in the thermodynamic limit) about $E=H$ and $\mathbf{Q}$ ($n=2$) is peaked at $E=H$. This is explained in Ref. 1 as a "kinematic effect." Since the total spin $\sum\mathbf{S}_j$ commutes with the exchange part of the Hamiltonian [Eq. (1)], the dynamic structure factor for $\mathbf{Q}=0$ consists of a δ function centered at $E=H$. For $\mathbf{Q}\sim 0$, the δ function broadens to a narrow peak.

The CEA results for the dynamic structure factor [Fig. 3(b)] are in better agreement than those for the density of the states. In the calculation of the dynamic structure factors we have used Eq. (17) of Ref. 1 with the imagi-

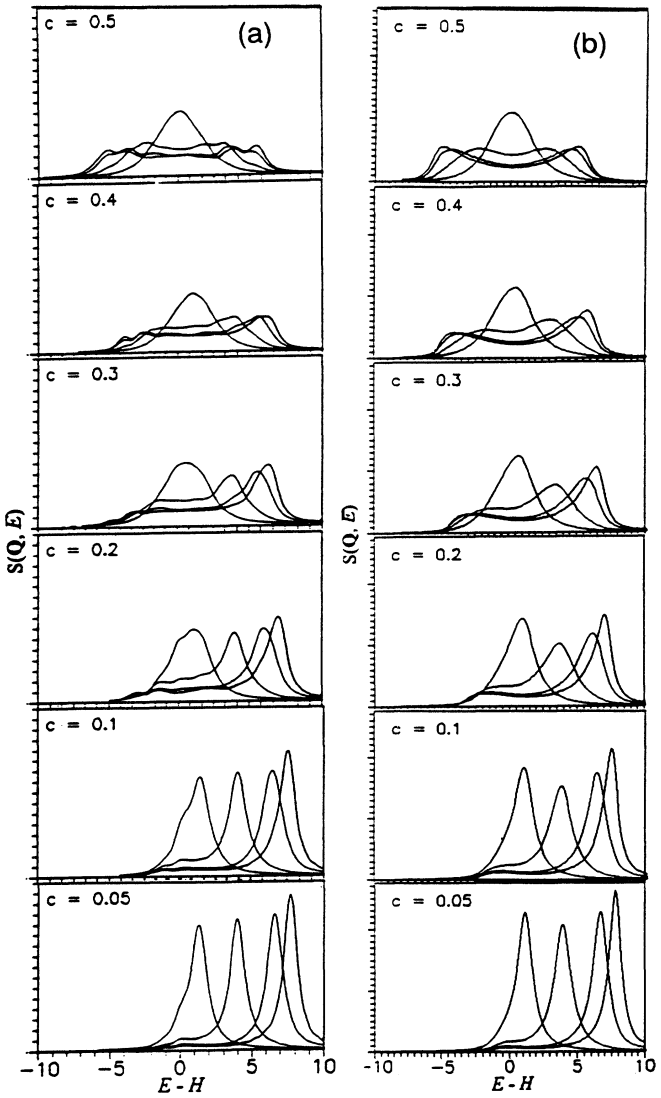

FIG. 3. (a) Dynamic structure factors for various values of c for the high-field limit. The curves from right to left correspond to $\mathbf{Q}=(\pi/8)(n,n)$ where $n=8$, 6, 4, and 2. Data are from a single configuration of a 24×24 array. (b) Dynamic structure factors obtained from the coherent-exchange approximation for various values of c. The curves from right to left correspond to $\mathbf{Q}=(\pi/8)(n,n)$ where $n=8$, 6, 4, and 2. All the curves have the same area, and energy is measured in units of J ($=S=1$).

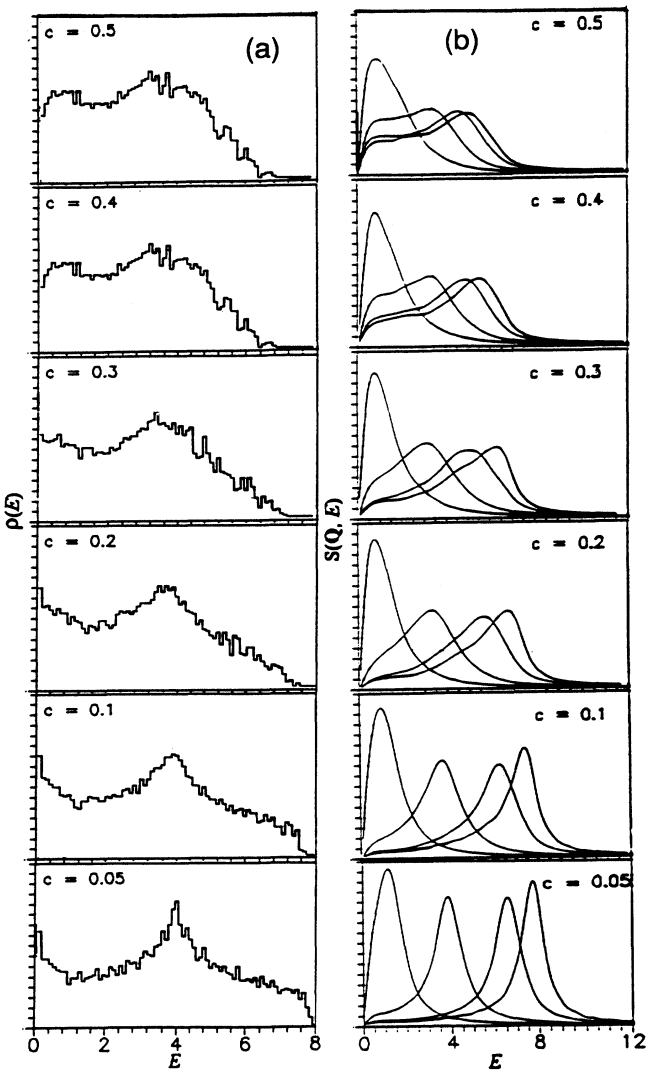

FIG. 4. (a) Histograms of the magnon density of states in zero field for various concentrations. Data are obtained from five configurations of a 24×24 array. All the histograms have the same area. (b) Dynamic structure factors for various values of c in zero field. The curves from right to left correspond to $\mathbf{Q}=(\pi/8)(n,n)$ where $n=8$, 6, 4, and 2. Data are from a single configuration of a 24×24 array. All the curves have the same area. Energy is measured in units of J ($=S=1$).

nary part of the energy equal to the cutoff value, 0.5 ($=\alpha$), and the **Q** values given above. The CEA successfully predicts the peak positions, the broadening of the peaks, and the shifts to the low-energy side of the spectrum. It also predicts tails which are developing into satellites as the disorder increases. For $c=0.5$, the peaks are symmetric about the point $E=H$.

III. SUMMARY AND DISCUSSION

In the high-field limit, we studied the two-dimensional spin glass both numerically and analytically. The CEA predicted qualitatively some features of the numerical data, e.g., the shift in the density of states towards the lower edge of the spectrum as the concentration increases and the positions and the widths of the peaks in the dynamic structure factors as well as the shift towards the low-energy side of the spectrum with the increasing disorder. The agreement between theory and data for the dynamic structure factor is very good. The CEA results for the density of states in three dimensions are in better agreement with the numerical data than those in two dimensions. This is because the approximate three-dimensional Green's function we used adds less error to the calculation of the coherent-exchange integral than that introduced by our approximate two-dimensional Green's function.

As the localization indices shown in Fig. 2 indicate, the modes with $E-H\gtrsim 0$ are weakly localized. Such a feature is predicted by the CEA method when $E=H$—the effective-medium limit of Ref. 4. For $E=H$, the coherent-exchange integral takes the form

$$J_c(E=H)=1-2c-i\sqrt{1-(1-2c)^2}\ . \tag{4}$$

For small wave vectors, the peaks in the dynamic structure factor are located at $E-H=\mathrm{Re}J_c(E=H)Q^2$ and have a half width at half height equal to $\mathrm{Im}J_c(E=H)Q^2$. One can define a magnon mean free path λ from the ratio of the group velocity V_g to the linewidth γ, i.e.,

$$\lambda=V_g/\gamma=[2\,\mathrm{Re}J_c(E=H)Q]/[\mathrm{Im}J_c(E=H)Q^2]$$
$$=2|1-2c|/[Q\sqrt{1-(1-2c)^2}]\ . \tag{5}$$

Thus, for $0<c<0.5$ and $0.5<c<1$, the magnons have finite mean free paths which diverge as $\mathbf{Q}\to 0$. For $c=0$, 1, the mean free paths are all infinite, whereas for $c=0.5$, the mean free paths at small **Q** are zero, since $\mathrm{Re}J_c(E=H)=0$.

The zero-field results for the density of states and the zero-temperature dynamic structure factor are shown in Figs. 4(a) and 4(b) over the same parameter ranges as in Figs. 1(a) and 3(a). The ground state is obtained from simulated quenching.[7] The histograms [Fig. 4(a)] indicate that for $c=0.05$, there is a peak at $E=4$ (which is a logarithmic singularity when $c=0$) which broadens as the concentration increases. With increasing c, the modes shift to $E=4$ from both the high- and low-energy sides. The dynamic structure factor data (Fig. 4(b)] show that the peaks broaden and shift towards low energies with increasing concentration of $-J$ bonds. Note that the peaks at $E\approx 0$ for $\mathbf{Q}=\pi/8(2,2)$ are an artifact of the simulation method (see Ref. 1).

In summary, the CEA gives qualitatively nearly as good an account of the behavior of the density of states and the zero-temperature dynamic structure factor of a spin glass in high fields in two dimensions as it did for the same quantities in three dimensions. However, it cannot be applied to a zero-field spin glass, whose ground state is frustrated. In the future, one looks to the development of a theory for the spin glass in zero field that works as well as the CEA does in the high-field limit.

ACKNOWLEDGMENTS

D.L.H. would like to thank Professor E. F. Shender for his stimulating interest in this problem. Computer time on the Cray X-MP was provided by the Office of Basic Energy Sciences of the Department of Energy. Additional support was provided by the National Science Foundation.

[1] I. Avgin, D. L. Huber, and W. Y. Ching, Phys. Rev. B **46**, 223 (1992).
[2] R. A. Tahir-Kheli, Phys. Rev. B **6**, 2808; **6**, 2826 (1972).
[3] I. Avgin and D. L. Huber, Phys. Rev. B **48**, 13 625 (1993).
[4] E. F Shender, J. Phys. C **11**, L423 (1978).
[5] A. Ghazali, P. Lallemand, and H. P. Diep, Physica **134A**, 628 (1986).
[6] E. N. Economou, *Green's Functions in Quantum Physics* (Springer-Verlag, Berlin, 1983).
[7] W. Y. Ching, D. L. Huber, and K. M. Leung, Phys. Rev. B **21**, 3708 (1980).